UDC 539.4

Hot Upset Studies on Sintered (Al–TiO_2–Gr) Powder Metallurgy Hybrid Composite

M. Ravichandran[a,1] and V. Anandakrishnan[b]

[a] Department of Mechanical Engineering, Chendhuran College of Engineering and Technology, Pudukkottai, Tamilnadu, India

[b] Department of Production Engineering, National Institute of Technology, Tiruchirappalli, Tamilnadu, India

[1] smravichandran@hotmail.com

УДК 539.4

Исследование горячей осадки спеченного гибридного композита Al–TiO_2–Gr, полученного методом порошковой металлургии

М. Равичандран[а], В. Анандакришнан[б]

[а] Чендуранский инженерно-технологический колледж, Пудуккоттай, Тамилнад, Индия

[б] Национальный технологический институт, Тируччираппалли, Тамилнад, Индия

Алюминиевые гибридные композиты Al+5%TiO_2, Al+5%TiO_2+2%Gr и Al+5%TiO_2+4%Gr из измельченных на грануляторе порошков синтезированы методом порошковой металлургии. Исследования методами сканирующей электронной микроскопии и энергодисперсионной рентгеновской спектроскопии показали, что упрочняющие добавки по объему образцов распределяются равномерно. Испытания на горячую осадку образцов, нагретых до 450°C, проведены с подробным изучением характеристик уплотнения и деформирования путем корреляции истинного осевого напряжения с истинной осевой деформацией, продольной деформацией и теоретической плотностью. Показано, что генерируемые в процессе горячей осадки напряжения увеличиваются при добавке графита в композит Al–TiO_2 и диоксида титана в Al без упрочняющих добавок. Выполнен анализ микроструктуры образцов после горячей осадки.

Ключевые слова: композиты с металлической матрицей, горячая осадка, напряжение, порошковая металлургия.

Introduction. Metal matrix composites (MMC) are under attention for many applications in aerospace, defense and automotive industries. Among MMCs, aluminum metal matrix composites are being considered as a group of new advanced materials for its light weight, high strength, low thermal expansion coefficient and good wear resistance [1]. In contrast, Al does not have enough tensile strength for many applications. Because of this weakness, ceramic particles (e.g., zircon) can be added for better hardness and tolerating high temperatures. Also, they can improve mechanical and tribological properties of the composite [2]. Recently, ceramics particulate reinforced metal matrix composites have been developed with promising results by several laboratories and companies. Despite the advantages listed above, particulate composites have not yet found a wide employment in the commercial applications because the hard particles embedded inside the matrix cause very serious problems in machining [3]. To avoid machining problems in composites,

© M. RAVICHANDRAN, V. ANANDAKRISHNAN, 2016

recently the hybrid composites are being developed. Ravindran et al. [4] suggested that the graphite particulates are well suited to this application, and their addition improves the machinability as well as wear resistance of Al–SiC composites. The use of TiO_2 as reinforcement in aluminum alloys has received a meager concentration although it possesses high hardness and modulus with superior corrosion resistance and wear resistance [5]. Large volume of literature is available on the synthesis of powder metallurgy aluminum composites using various reinforcements such as TiB_2 [6], AlN [7], glass [8], graphene nano sheets [9], Si [10], MgH_2 [11], Al_3Ti [12], B_4C [13], BN [14], Fe [15], carbon nano tubes [16], Ni_3Al [17], fly ash [18], Al_2O_3 [19], $ZrSiO_4$ [2], SiC [20], $MoSi_2$ [21] however very little attention has been given to the TiO_2 reinforced composites through powder metallurgy route.

Automotive manufacturers are always looking for new ways to reduce the weight of vehicle components. The powder metallurgy (PM) process has become a considerable interest in recent years. PM technique has been a traditional method of manufacturing MMC materials and components [22]. Powder processes are more flexible than casting and forging techniques, they are used in a wide range of industries, from automotive and aerospace applications to power tools and household appliances [23]. The plastic deformation of sintered powder preforms is similar to that of conventional fully dense materials, but there are additional complications due to the substantial volume fraction of voids in the preform. In particular, the voids must be eliminated by the application of metal forming processes such as extrusion, forging, upset and coining [24]. Hot forging of sintered aluminum preforms can also impart significant mechanical gains in terms of properties [25]. In isothermal upset forging of pure aluminum, the change in the contact condition and the lubricant behavior were evaluated by continuously measuring the ultrasonic reflection intensity from the contact interface between the tool (die) and workpiece [26]. Forging behavior of 2124 aluminum alloy containing 26 vol.% of SiC particles was investigated at room and elevated temperature tensile tests. The results obtained were utilized to define the forging parameters. The material exhibited excellent forgeability and after forging the tested composite was found to be crack free. This feature is very likely due to the size of the reinforcing SiC particles, smaller than those generally used for conventional metal/ceramic composite processing. Furthermore, forging resulted in an increase of both tensile strength and ductility with respect to the as-fabricated condition [27]. Composites of an aluminum–silicon alloy containing different volume fractions of particulate silicon carbide reinforcement and unreinforced matrix alloy samples were produced by the permanent die casting technique. After forging, the yield strength of the matrix alloy and composite samples was increased by about 80%, and the improvement in tensile strength was about 40%. The addition of increasing amounts of particulate SiC decreased the ductility and increased the yield and tensile strength [28]. The mechanical response of AA2618 aluminum based metal matrix composite was investigated by means of hot compression tests. The flow stress curves were obtained in the temperature and strain rate ranges of 350–500°C and $1–10^{-3}$ s^{-1}, respectively in order to obtain the processing and stability maps of the studied material following the dynamic material model [29]. Forming behavior of Al–TiO_2–Gr hybrid composites (Al+2.5%TiO_2+2%Gr, Al+2.5%TiO_2+4%Gr, Al+5%TiO_2+ +2%Gr, and Al+5%TiO_2+4%Gr) during cold upset under plane stress state conditions and EDAX, XRD, and SEM analysis of the ball milled powders also reported in the previous studies [30, 31].

The present work aims to study the behavior of unreinforced Al, Al+5%TiO_2 composites, and Al+5%TiO_2+2%Gr and Al+5%TiO_2+4%Gr hybrid composites during hot upset. The hot upset studies were carried out for all the sintered preforms by correlating true axial stress with true axial strain, lateral strain and percentage theoretical density. In this paper the results of SEM and EDAX analysis for the sintered preforms were reported. Microstructure analyses for the hot forged samples are also presented.

1. **Experimental Details**. Atomized aluminum (Al) powder of 99.7% purity was used for the matrix material and rutile phase of titanium-di-oxide (TiO_2) and graphite (Gr) powders are used as reinforcement materials. The reinforcement materials (TiO_2) and (Gr) are blended with matrix material (Al) in the weight percentages to yield the different composites namely, Al+0%TiO_2, Al+5%TiO_2, Al+5%TiO_2+2%Gr, and Al+5%TiO_2+4%Gr for the present work.

The compaction process setup is shown in Fig. 1 and Fig. 2a and 2b shows the green compact before and after ceramic coating. The details of blending, compaction, ceramic coating and sintering process were well explained in previous reports [31]. The sintered preforms were cleaned and measurements such as initial height (H_0), diameter (D_0), and mass (m) were carried out. Cylindrical compressive specimens 24 mm in diameter and 12 mm in height were machined from those sintered billets. Hot upset tests were conducted in the temperature range of 450℃ in step of 25℃. Graphite lubricant was used to ensure homogeneous deformation during hot upset. The specimens were heated at 20℃/min up to the deformation temperature, held for 10 min and then compressed. In experimental process, the computer-processor of Venus instruments collected the data automatically and obtained true stress–strain curves using standard equations. Deformed specimens were water quenched. The density of the hot forged sample was determined using Archimedes principles.

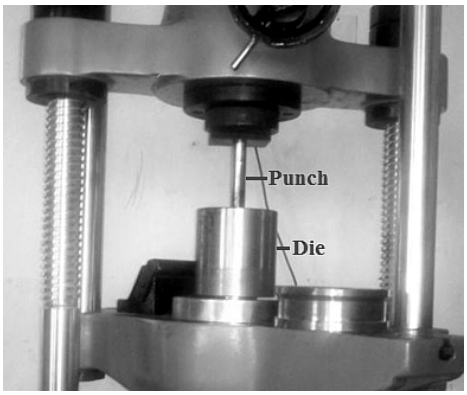

Fig. 1. Photograph showing compaction process.

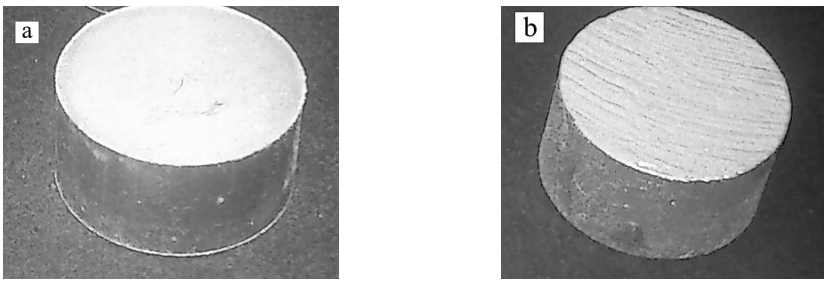

Fig. 2. Photograph showing green compact (a) and compact after ceramic coating (b).

The microstructure analysis of sintered composite preforms was investigated by scanning electron microscope (SEM) using JEOL JSM-35 CF SEM instrument. Compositional analysis of the Al, TiO_2, and Gr sintered composite preforms was analyzed by energy dispersive analysis using X-ray (make: EDAX-AMETEK-TSL). Microstructures of hot forged samples were analyzed using optical microscope (De-Wintor Inverted Trinocular Metallurgical Microscope with Material plus version-2 software).

2. **Results and Discussion**.

2.1. ***SEM Analysis of Sintered Composite Preforms***. SEM photograph of the sintered preforms are shown in Fig. 3. The morphology of the sintered Al preform is shown in Fig. 3a. Figure 3b shows the uniform distribution of TiO_2 particles in the Al matrix. It can be seen that the TiO_2 particles distributed evenly within the Al boundary and there is no agglomeration of TiO_2. In Fig. 3c and 3d, it can be seen, that the uniform distribution of graphite in the Al+5%TiO_2 sintered composite preforms and also observed that the matrix and reinforcements interfacial bindings are good in agreement.

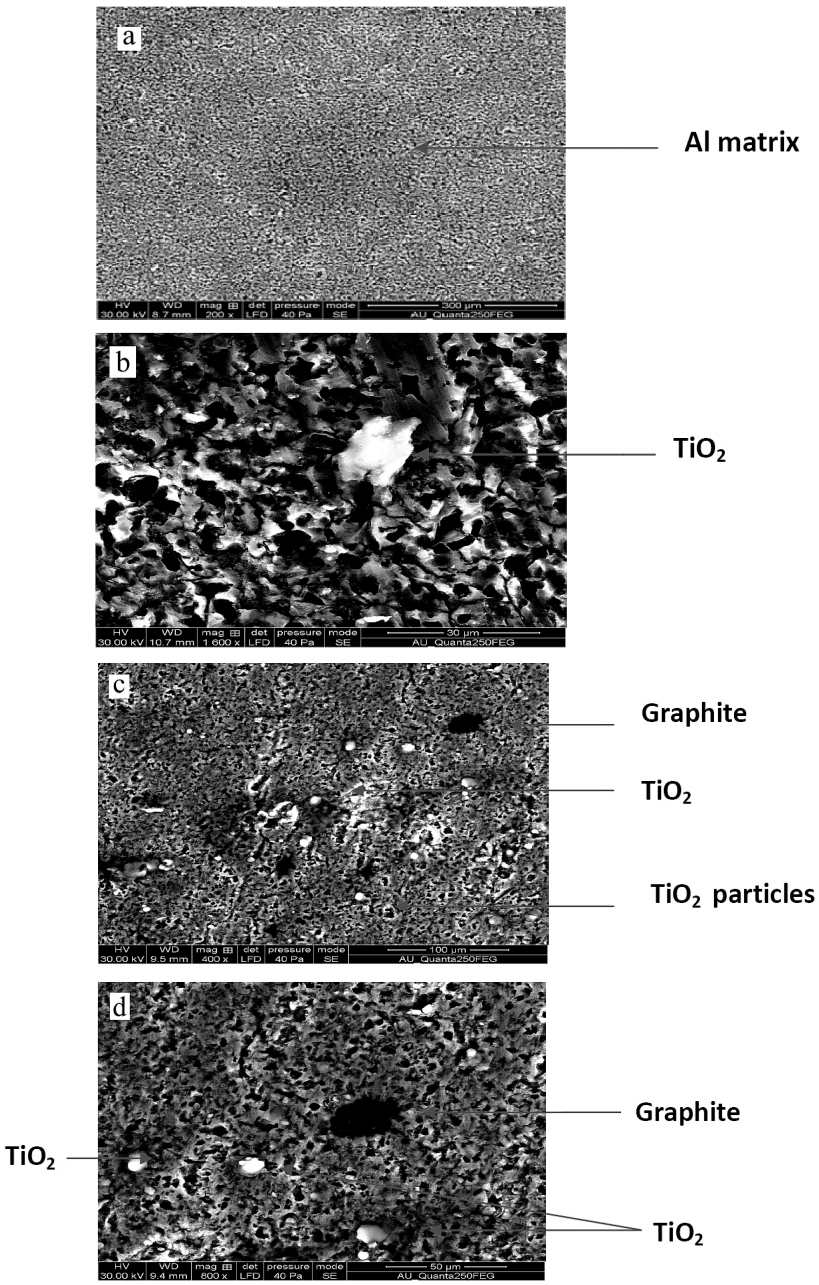

Fig. 3. SEM images of sintered (a) Al preform, (b) Al+5%TiO_2 composite, (c) Al+5%TiO_2+2%Gr, and (d) Al+5%TiO_2+4%Gr hybrid composite preforms.

2.2. ***EDAX of Sintered Composite Preforms***. Figure 4 shows the EDAX spectrum of the sintered Al, Al+5%TiO_2, Al+5%TiO_2+2%Gr and Al+5%TiO_2+4%Gr sintered preforms as an example of confirmation for the presence of oxide and titanium phases in Al phase. Figure shows the appearance of peaks corresponding to the presence of Al, TiO_2, and graphite. Large number of peaks with highest intensity is pertained to Al who confirms the major content is Al. The observed weight percentage of titanium dioxide content reveals that, it is well incorporated into Al matrix.

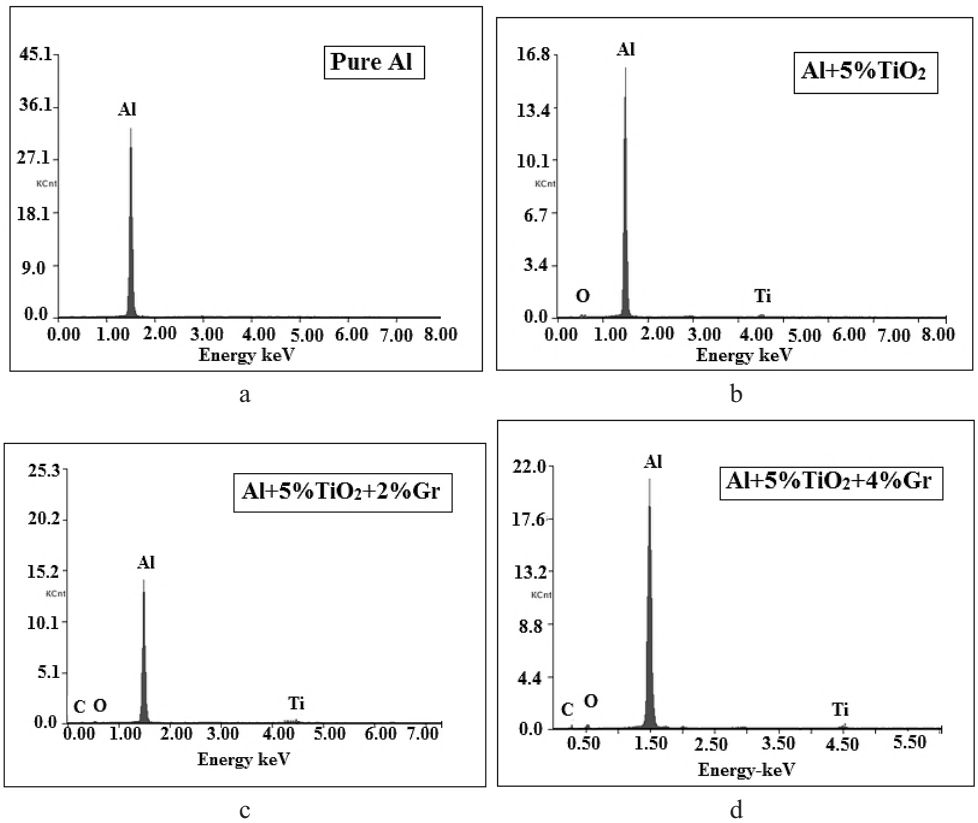

Fig. 4. EDAX of sintered (a) Al, (b) Al+5%TiO_2 composite, (c) Al+5%TiO_2+2%Gr, and (d) Al+5%TiO_2+4%Gr hybrid composite preforms.

2.3. ***Hot Upset Studies***.

2.3.1. *True Axial Stress versus True Axial Strain*. Figure 5 shows the graph drawn between true axial stress and true axial strain of Al, Al+5%TiO_2, Al+5%TiO_2+2%Gr, and Al+5%TiO_2+4%Gr preforms to study the deformation during hot upset. It clearly understands from the graph, initially true axial stress required is more for lower rate of deformation. Among the different preforms, the sintered unreinforced Al exhibits the largest level of deformation at lowest axial stress values. Addition of 5%TiO_2 to the Al matrix and 2 and 4% of graphite to the Al+5%TiO_2 composite requires more applied stress than the stress required for pure Al preforms at any stage of deformation. The sintered composite preforms contain 5% titanium dioxide and 4% graphite needed more applied load for the same level of deformation. Hence it is understand that, the addition of reinforcement resists the plastic deformation during hot upset. The hard as well as soft reinforcement is surrounded in the soft Al matrix resulting greater resistance to plastic deformation.

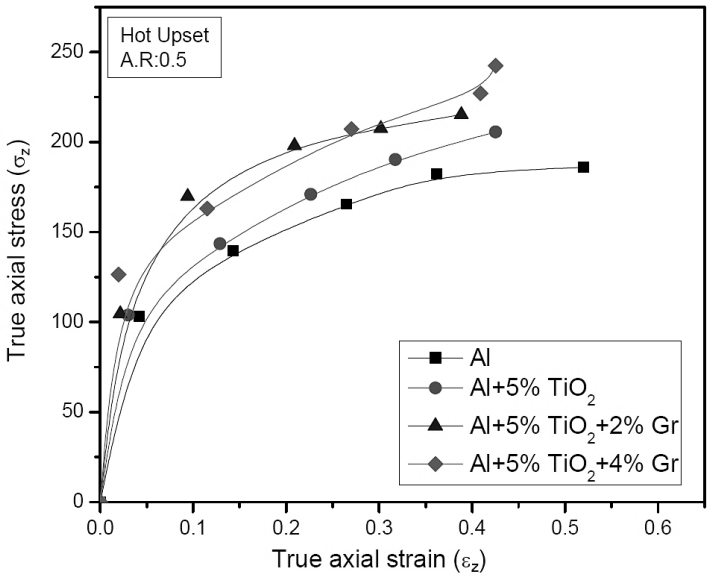

Fig. 5. Plots of true axial stress versus true axial strain.

2.3.2. *True Axial Stress versus Lateral Strain*. Figure 6 shows the plot between true axial stress and lateral strain for Al, Al+5%TiO_2, Al+5%TiO_2+2%Gr, and Al+5%TiO_2+4%Gr preforms. It clearly understands from these curves, the lateral deformation trend is similar to that observed for axial deformation. But the value of lateral strain is smaller than the true axial strain and it could be understood that the lateral deformation is lower than the axial deformation for Al+5%TiO_2, Al+5%TiO_2+2%Gr, and Al+5%TiO_2+4%Gr composites than unreinforced Al preform. Better lateral deformation was observed for the unreinforced Al preforms and the addition of TiO_2 to the Al matrix and addition of graphite to the Al+5%TiO_2 composite affects the both axial and lateral deformation of the composites.

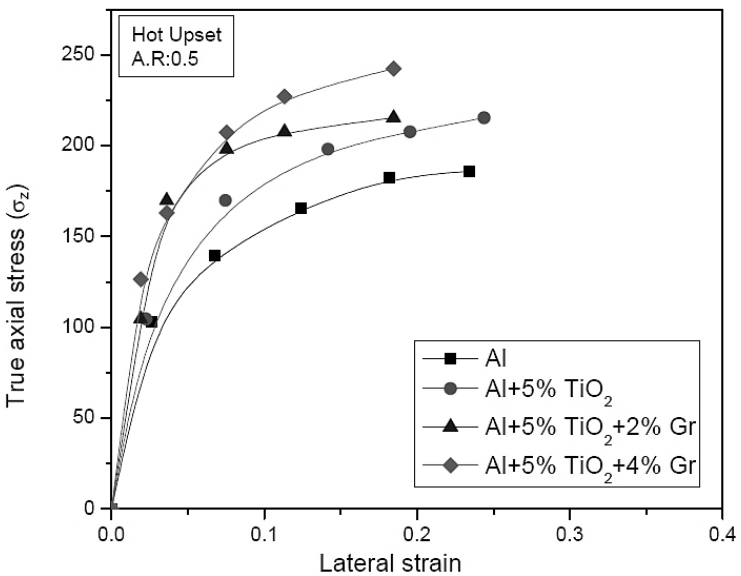

Fig. 6. Plots of true axial stress versus lateral strain.

2.3.3. *True Axial Stress versus Percentage Theoretical Density*. Figure 7 shows the variation of percentage theoretical density with respect to true axial stress for the preforms containing various weight percentages of TiO_2 and Gr during hot upset. The better densification was observed for the unreinforced Al preforms for the lowest applied load. Addition of 5 wt.% of TiO_2 to the Al matrix decreases the densification and requires more applied load. In the same way, the addition of 2 and 4 wt.% of graphite to the Al+5%TiO_2 composite decreases the densification and further the required applied true axial stress increases. In the case of unreinforced Al preforms the presence of pores are deformed during hot upset however for the composite preforms, the pores are occupied by the (TiO_2 and Gr) reinforcements and it resists the deformation and requires a higher applied stress for the further densification. The poor densification was observed for the Al+5%TiO_2 composite containing 4 wt.% of Gr as compared to the unreinforced Al preform.

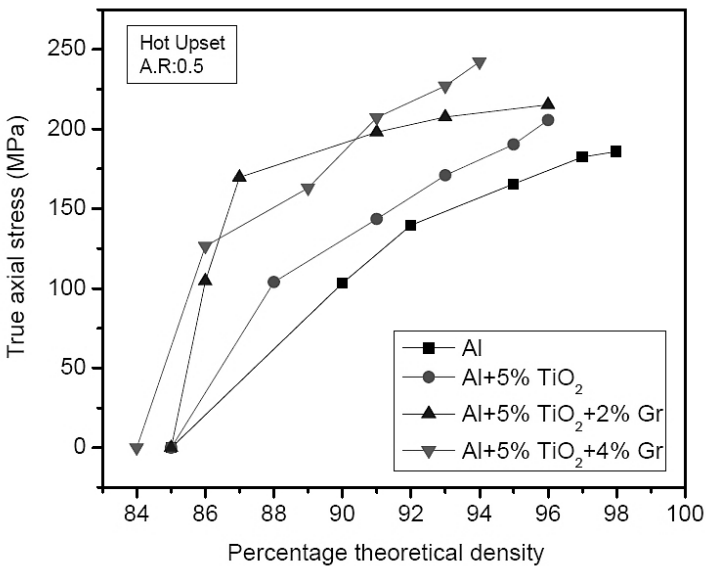

Fig. 7. Plots of true axial stress versus percentage theoretical density.

2.3.4. *Percentage Theoretical Density versus True Axial Strain*. Figure 8 shows the plots of percentage theoretical density versus true axial strain to study the densification and deformation behavior of the preforms during hot upset. The trend observed for all the preforms are similar and the better densification and deformation was observed for the unreinforced Al. Addition of TiO_2 and Gr to the unreinforced Al matrix decreases the densification and deformation due to the matrix work hardening.

It was observed during hot upset that, some of the tested composites were cracked. Therefore, the ductile-brittle transition behavior was taken in consideration. Thus, fractographs of different deformed composites at are shown in Fig. 9. The addition of reinforcements caused circumferential cracks and the crack width increased with increasing weight fraction of TiO_2 and Gr reinforcements (Fig. 10). The similar results were obtained by Abouelmagd during hot deformation and wear resistance studies of Al–Al_2O_3 PM composites [32].

2.3.5. *Microstructure Analysis of Hot Upset Samples*. Microstructures of composites with the content of 5%TiO_2 and 2 and 4 wt.% Gr, hot upset at 450°C are shown in Fig. 11. Because of difference between the densities of TiO_2 and Al, the contrast of the micrographs is high enough for further investigations. Al matrix and bright particles of TiO_2 can be clearly observed. The phases are indicated by arrows on the above images. It should be

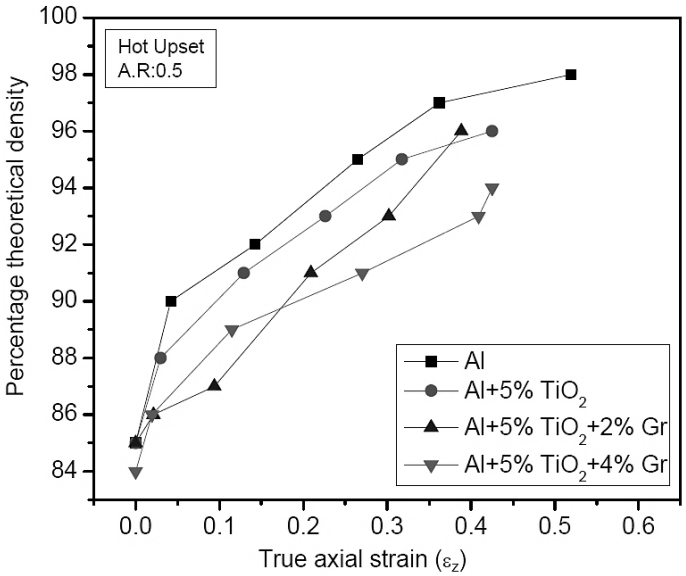

Fig. 8. Plots of percentage theoretical density versus true axial strain.

a b c d

Fig. 9. Photograph showing (a) Al, (b) Al+5%TiO_2, (c) Al+5%TiO_2+2%Gr, and (d) Al+5%TiO_2+4%Gr PM preform after hot upset.

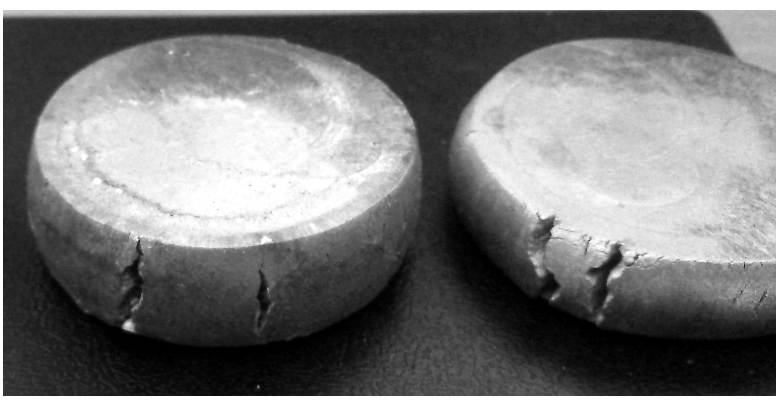

Fig. 10. Fractography of Al+5%TiO_2 composite and Al+5%TiO_2+4%Gr hybrid composite.

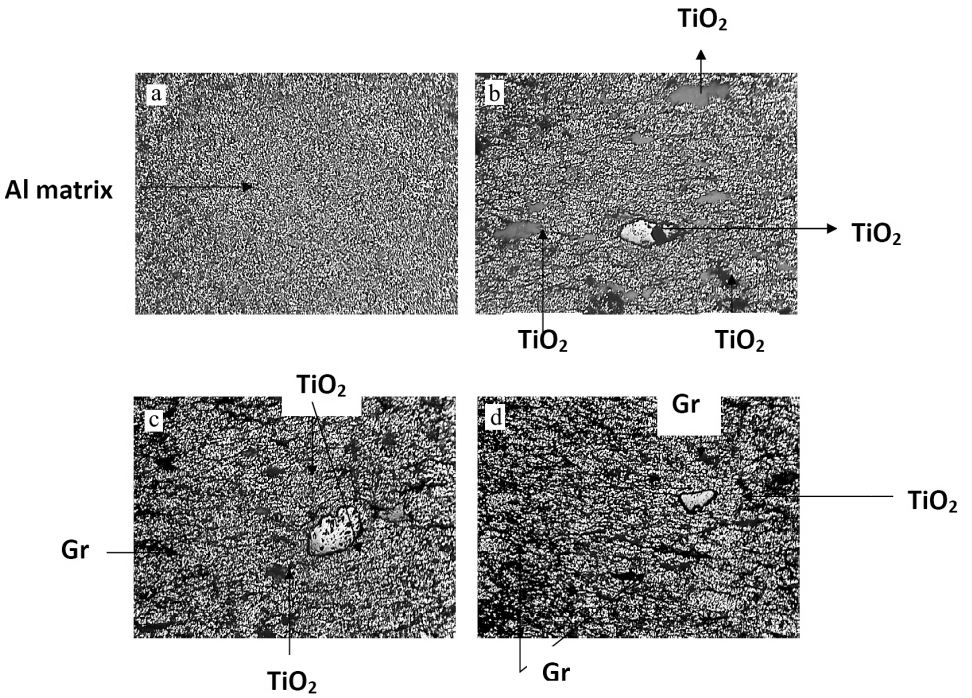

Fig. 11. Microstructure of (a) Al, (b) Al–5%TiO_2, (c) Al–5%TiO_2–2%Gr, and (d) Al–5%TiO_2–4%Gr hot forged preforms.

noted that micron size TiO_2 particles were well dispersed in the matrix of Al and just a partial agglomeration in composites with high content of TiO_2 can be detected in Fig. 11b. As demonstrated, there are some black points representing the presence of graphite in the composites. On the other hand, increasing the volume percent of TiO_2 and Gr particles decreases the uniformity and homogeneity of the samples, and the number of TiO_2 and Gr clusters tends to increase. The reason for fine distribution of reinforcement particles is to determine the appropriate time and method of mixing.

Conclusions. Aluminum matrix composites composed of TiO_2 and Gr as reinforcements were synthesized by the powder metallurgy method. The hot upset studies had been carried out and the following conclusions are drawn:

1. SEM and EDAX analysis of sintered preforms show the distribution of the reinforcements (TiO_2 and Gr) with the matrix material is homogeneous.

2. Hot upset studies reveal that the maximum true axial stress and minimum axial strain obtained for hybrid composite preforms are higher than those in unreinforced Al preform.

3. Addition of TiO_2 and Gr reinforcements to the Al matrix decreases the densification and deformation (both axial and lateral) during hot upset.

4. The addition of TiO_2 and Gr causes the ductile-brittle transition phenomenon of the investigated composites. The crack width increases with weight percentage of reinforcements.

Р е з ю м е

Алюмінієві гібридні композити Al+5%TiO_2, Al+5%TiO_2+2%Gr й Al+5%TiO_2+4%Gr із подрібнених на грануляторі порошків синтезовані методом порошкової металургії. Дослідження методами сканувальної електронної мікроскопії та енергодисперсійної

рентгенівської спектроскопії показали, що зміцнювальні домішки по об'єму зразка розподіляються рівномірно. Випробування на гарячу осадку нагрітих до 450°C зразків проведено з детальним вивченням характеристик ущільнення і деформування шляхом кореляції істинного осьового напруження з істинною осьовою деформацією, поздовжньою деформацією і теоретичною щільністю. Показано, що генеруючі в процесі гарячої осадки напруження збільшуються при додатку графіту в композит Al–TiO_2 і диоксиду титану в Al без зміцнювальних домішок. Виконано аналіз мікроструктури зразка після гарячої осадки.

1. R. Derakhshandeh Haghighi and A. Jenabali Jahromi, "An investigation on the capability of equal channel angular pressing for consolidation of aluminum and aluminum composite powder," *Mater. Design*, **32**, 3377–3388 (2011).
2. H. Abdizadeh, Maziar Ashuri, Pooyan Tavakoli Moghadam, et al., "Improvement in physical and mechanical properties of aluminum/zircon composites fabricated by powder metallurgy method," *Mater. Design*, **32**, 4417–4423 (2011).
3. Mohammed T. Hayajneh, Adel Mahmood Hassan, and Ahmad Turki Mayyas, "Artificial neural network modeling of the drilling process of self-lubricated aluminum/alumina/graphite hybrid composites synthesized by powder metallurgy technique," *J. Alloy Compd.*, **478**, 559–565 (2009).
4. P. Ravindran, K. Manisekar, P. Narayanasamy, et al., "Application of factorial techniques to study the wear of Al hybrid composites with graphite addition," *Mater. Design*, **39**, 42–54 (2012).
5. S. Sivasankaran, K. Sivaprasad, R. Narayanasamy, and Vijay Kumar Iyer, "An investigation on flowability and compressibility of AA 6061 100–x-x wt.% TiO_2 micro and nanocomposite powder prepared by blending and mechanical alloying," *Powder Technol.*, **201**, 70–82 (2010).
6. M. Karbalaei Akbari, H. R. Baharvandi, and K. Shirvanimoghaddam, "Tensile and fracture behavior of nano/micro TiB_2 particle reinforced casting A356 aluminum alloy composites," *Mater. Design*, **66**, 150–161 (2015).
7. Hamid Abdoli, Ehsan Saebnouri, S. K. Sadrnezhaad, et al., "Processing and surface properties of Al–AlN composites produced from nanostructured milled powders," *J. Alloy Compd.*, **490**, 624–630 (2010).
8. K. U. Kainer and B. L. Mordike, "Creep properties of powder metallurgically produced aluminium-glass composites," in: H. J. McQueen, J.-P. Bailon, and J. I. Dickson (Eds.), Strength of Metals and Alloys (ICSMA 7), Proc. of the 7th Int. Conf. on *Strength of Metals and Alloys* (August 12–16, 1985, Montreal, Canada), pp. 761–766.
9. J. Wang, Z. Li, G. Fan, et al., "Reinforcement with graphene nanosheets in aluminum matrix composites," *Scripta Mater.*, **66**, 594–597 (2012).
10. G. Miranda, M. Buciumeanu, O. Carvalho, et al., "Interface analysis and wear behavior of Ni particulate reinforced aluminum–silicon composites produced by PM," *Composites Part B: Eng.*, **69**, 101–110 (2015).
11. A. Glage, R. Ceccato, I. Lonardelli, et al., "A powder metallurgy approach for the production of a MgH_2–Al composite material," *J. Alloy Compd.*, **478**, 273–280 (2009).
12. V. Abbasi Chianeh, H. R. Madaah Hosseini, and M. Nofar, "Micro structural features and mechanical properties of Al–Al_3Ti composite fabricated by in-situ powder metallurgy route," *J. Alloy Compd.*, **473**, 127–132 (2009).

13. Temel Varol, Aykut Canakci, and Sukru Ozsahin, "Artificial neural network modeling to effect of reinforcement properties on the physical and mechanical properties of Al2024–B_4C composites produced by powder metallurgy," *Composites Part B: Eng*., **54**, 224–233 (2013).
14. Maho Yamaguchia, Fanqiang Meng, Konstantin Firestein, et al., "Powder metallurgy routes toward aluminum boron nitride nanotube composites, their morphologies, structures and mechanical properties," *Mater. Sci. Eng. A*, **604**, 9–17 (2014).
15. R. Narayanasamy, T. Ramesh, and K. S. Pandey, "Some aspects on cold forging of aluminium–iron powder metallurgy composite under triaxial stress state condition," *Mater. Design*, **29**, 891–903 (2008).
16. Z. Y. Liu, B. L. Xiao, W. G. Wang, and Z. Y. Ma, "Tensile strength and electrical conductivity of carbon nanotube reinforced aluminum matrix composites fabricated by powder metallurgy combined with friction stir processing," *J. Mater. Sci. Technol*., **30**, 649–655 (2014).
17. Y. Wang, W. M. Rainforth, H. Jones, M. Lieblich, "Dry wear behaviour and its relation to microstructure of novel 6092 aluminium alloy–Ni_3Al powder metallurgy composite," *Wear*, **251**, 1421–1432 (2001).
18. E. Marin, M. Lekka, F. Andreatta, et al., "Electrochemical study of aluminum–fly ash composites obtained by powder metallurgy," *Mater. Charact.*, **69**, 16–30 (2012).
19. Majed Zabihi, Mohammad Reza Toroghinejad, and Ali Shafyei, "Application of powder metallurgy and hot rolling processes for manufacturing aluminum/alumina composite strips," *Mater. Sci. Eng. A*, **560**, 567–574 (2013).
20. A. Hassani, E. Bagherpour, and F. Qods, "Influence of pores on workability of porous Al/SiC composites fabricated through powder metallurgy + mechanical alloying," *J. Alloy Compd.*, **591**, 132–142 (2014).
21. J. Corrochano, M. Lieblich, and J. Ibáñez, "The effect of ball milling on the microstructure of powder metallurgy aluminium matrix composites reinforced with $MoSi_2$ intermetallic particles," *Composites Part A: Appl. Sci. Manuf.*, **42**, 1093–1099 (2011).
22. L. F. Guleryuz, S. Ozan, D. Uzunsoy, and R. Ipek, "An investigation of the microstructure and mechanical properties of B_4C reinforced PM magnesium matrix composites," *Powder Metall. Metal Ceram.*, **51**, 456–462 (2012).
23. S. Li, H. Imai, K. Kondoh, et al., "Dependence of microstructure and mechanical properties on hot-extrusion temperatures of the developed high-strength Cu40Zn–CrFeTiSn brassby powder metallurgy," *Mater. Sci. Eng. A*, **558**, 616–622 (2012).
24. R. Narayanasamy and K. S. Pandey, "A study on the barrelling of sintered iron preforms during hot upset forging," *J. Mater. Process. Technol.*, **100**, 87–94 (2000).
25. R. E. D. Mann, R. L. Hexemer, Jr, I. W. Donaldson, and D. P. Bishop, "Hot deformation of an Al–Cu–Mg powder metallurgy alloy," *Mater. Sci. Eng. A*, **528**, 5476–5483 (2011).
26. Hiroyuki Saiki, Zhi Hong Zhan, Yasuo Marumo, et al., "Evaluation of contact conditions in hot forging of pure aluminum using ultrasonic examination," *J. Mater. Process. Technol.*, **177**, 243–246 (2006).
27. C. Badini, G. M. La Vecchia, P. Fino, and T. Valente, "Forging of 2124/SiC_p composite: preliminary studies of the effects on microstructure and strength," *J. Mater. Process. Technol.*, **116**, 289–297 (2001).
28. Ismail Özdemir, Ümit Cöcen, and Kazim Önel, "The effect of forging on the properties of particulate-SiC-reinforced aluminium-alloy composites," *Compos. Sci. Technol*., **60**, 411–419 (2000).

29. P. Cavaliere, E. Cerri, and P. Leo, “Hot deformation and processing maps of a particulate reinforced 2618/Al_2O_3/20p metal matrix composite,” *Compos. Sci. Technol*., **64**, 1287–1291 (2004).

30. M. Ravichandran, A. Naveen Sait, and V. Anandakrishnan, “Synthesis and forming behavior of aluminium-based hybrid powder metallurgic composites,” *Int. J. Min. Metall. Mater.*, **21**, 181–189 (2014).

31. M. Ravichandran, A. Naveen Sait, and V. Anandakrishnan, Densification and deformation studies on powder metallurgy Al–TiO_2–Gr composite during cold upsetting,” *J. Mater. Res.*, **29**, 1480–1487 (2014).

32. G. Abouelmagd, “Hot deformation and wear resistance of P/M aluminium metal matrix composites,” *J. Mater. Process. Technol.*, **155-156**, 1395–1401 (2004).

Received 09. 06. 2015